

THE INTERACTIONS BETWEEN PAHs AND MINERALS

Heiam Hamed, William Hale, Ben Stern
School of Archaeological and Forensic Sciences,
University of Bradford, UK

Abstract— Abstract Trials using iodine as a marker for PAHs showed there were notable interactions between the minerals and PAHs, with calcium carbonate absorbing PAHs much more than silica. The interaction between PAH compounds and minerals in the soil was determined using iodine with the SEM technique in some method development studies; from the results obtained there was an interaction between PAH compounds and minerals, but the method shows only that there is an interaction but does not determine the quantity of organic compounds present.

Keywords— PAH, Soil, minerals, and interactions.

I. INTRODUCTION

The introduction Polycyclic aromatic hydrocarbons (PAHs) are organic compounds containing carbon and hydrogen with two or more fused aromatic rings [1]. Sixteen PAHs have been listed by the United States Environmental Protection Agency as priority pollutants due to their toxicity and carcinogenic behaviour [2]. PAHs are found individually or as a complex mixture. These compounds originate from anthropogenic and natural processes[2]. Most anthropogenic PAHs are produced through the incomplete combustion of carbonaceous materials, for example, coal, diesel, and petrol[3]. The main sources of natural PAHs are volcanic eruptions and natural fires. Without anthropogenic input the background concentrations of PAHs in soils are reported to be 1 - 10 ng/g [4]. PAHs in the atmosphere deposit in soil through wet or dry deposition processes. In wet sediments, PAHs dissolve in precipitation, while dry sediment deposition occurs when the compounds are deposited on the soil as dry particles or gases [5]. Soil contamination of PAH could have a direct impact on public health [6]. Soil pollution with PAHs can easily be delivered to humans from direct contact or suspended dust [7],[8]. The soil is one of the most important sources of storage and re-emission of PAHs.

The work of Goldenberg et al. (2014) was based on the reaction between unsaturated organic compounds and iodine. In a closed glass chamber, powdered ceramic samples were placed with a few iodine crystals and then exposed to iodine vapour. Iodine has a high vapour pressure at room temperature resulting in the chamber being rapidly saturated with iodine vapour [9]. The iodine will bind only to the carbon-carbon

unsaturated bonds and not to the carbon-carbon single bonds, the concentration of iodine, and therefore saturated molecules can then be determined by X-ray fluorescence [9].

Goldenberg et al. (2014) used the above principle in two ways. First, they assessed the amount of unsaturated fatty acids and the state of general preservation of organic materials to identify appropriate samples for the analysis of organic residues in ceramic samples. The second method was based on the interaction of iodine with saturated bonds to visualize the distribution of unsaturated molecules of organic materials on the ceramic surfaces [9].

Based on the work by Goldenberg et al. (2014), two new methods have been developed. This experiment was designed to determine the interactions between PAHs and minerals using iodine absorption and scanning electron microscopy X-ray fluorescence. This was carried out using the measurement of iodine as a proxy for where PAHs interact with the minerals [9].

II. DETAILS EXPERIMENTAL

A. Materials and Procedures

An agate pestle and mortar was used to grind and homogenise each test sample (soil, calcite, silica). 1 g of each was placed into a glass scintillation vial. A small amount of each sample was placed on SEM-stubs (0.5" aluminium with sticky mounting tape).

0.1 g of individual PAH standard (naphthalene) was weighed and transferred into a 100 ml volumetric flask, hexane was used to dissolve the PAH. The volumetric was then filled to the mark to make a 1 mg/ml solution.

Each test sample (e.g. calcium carbonate) was put in a flask and then was spiked with 1 ml of the 1 mg/ml PAH solution. The solutions did not cover the solid sample therefore 1 ml of hexane was further added to cover the sample and to ensure a homogenous coating.

B. Exposure of Samples to I₂ Vapour

The samples on SEM-stubs were placed equidistant from a vial containing a few crystals of solid iodine in a desiccator jar. The lid was removed from the vial containing the iodine and the desiccator lid replaced (all within a fume cupboard). The samples were exposed to I₂ vapour for 4 hours at room temperature.

Initially the room temperature was too cool to enable iodine sublimation and for this reason the samples did not adsorb iodine. Therefore, to know the correct temperature to use iodine was placed in a vial and then heated whilst monitoring the temperature using a thermometer. At 21 °C sufficient sublimation was observed with a purple vapour present in the vial and deposits of solid purple iodine crystals on the vial walls. The temperature of 21°C was chosen for use in subsequent experiments because at this temperature the iodine appeared to have been sufficient sublimated.

C. Scanning Electron Microscopy and X-ray Fluorescence Analysis

The samples were coated with carbon by using an Emitech-k450. This was done to remove weakly bound iodine during the vacuum deposition and to create a conductive surface for SEM.

The samples were analysed for the presence of iodine by using scanning electron microscopy with X-ray fluorescence (FEI QUANTA 400) with Oxford Inca FDX detector V3.30 using a backscattered electron BSE detector.

Energy Dispersive X-ray (EDX) analyses were achieved at 20 kV with a distance of 11 mm.

The calibration of EDX was achieved using a cobalt standard. The iodine was mapped using Inca software.

III. RESULTS AND DISCUSSION

A. Justification for different PAHs with different concentrations

After the use of oleic acid, other organic samples were selected; acenaphthlene, anthracene and phenathrene, again examples of 3 ring PAHs.

1g acenaphthlene, 0.2 g anthracene and 1g phenathrene were separately weighed into glass scintillation vials and 3, 15 and 5 ml of DCM/MeOH 2:1 (v/v) respectively were used to dissolve each. Separate 0.5 g of calcium carbonate samples were weighed into glass scintillation vials and separate 2 ml of the above solutions were then added (1 ml of the acenaphthlene solution). The samples were mixed well and the samples left in a fume cupboard to enable the DCM/MeOH to evaporate to dryness. The samples were analysed by SEM-XRF as described above.

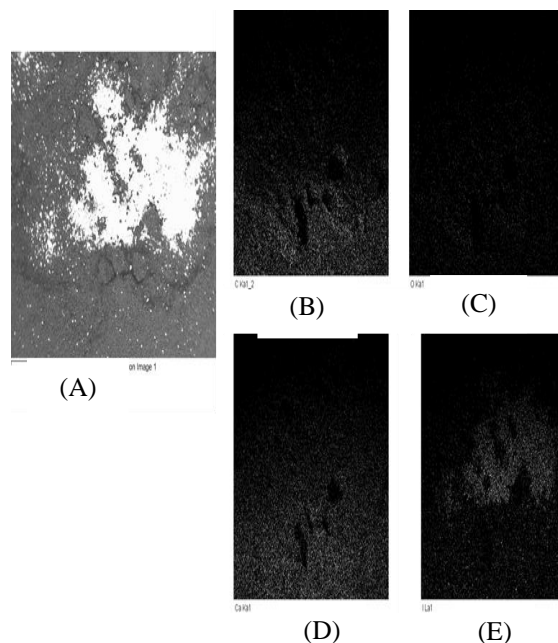


Fig 1. Backscattered electron image of anthracene with calcium carbonate exposed to iodine for 4 hr at 21 °C with magnifications 30x (A). Distribution map of carbon (B), distribution map of oxygen (C), distribution map of calcium (D) and distribution map of iodine (E).

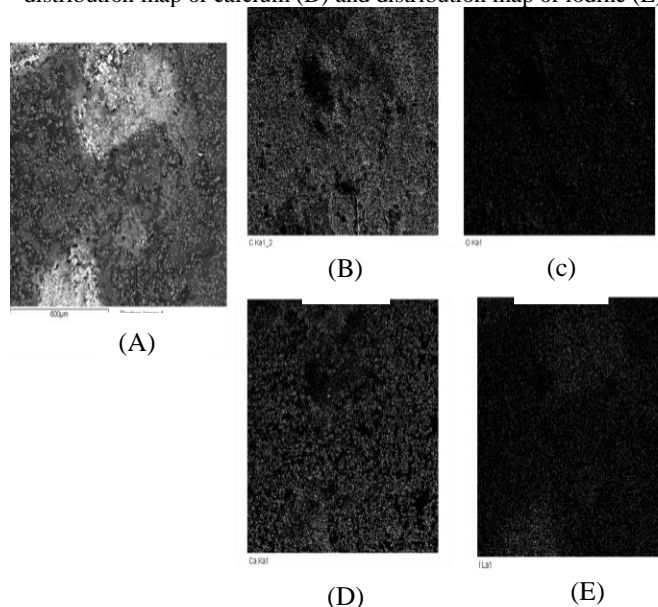


Fig 2. Backscattered electron image of phenathrene with calcium carbonate exposed to iodine for 4 hr at 21 °C with magnifications 30x (A). Distribution map of carbon (B), distribution map of oxygen (C), distribution map of calcium (D) and distribution map of iodine (E).

B. Oleic acid to confirm iodine absorption

In this method 0.3 g of oleic acid was weighed into a glass scintillation vial and 1ml of DCM/MeOH 2:1 (v/v) was used to make a solution. 0.5 g of calcium carbonate was weighed in a glass scintillation vial, and 1 ml of the solution of oleic acid then added. The sample was well mixed and left in a fume cupboard to enable the DCM/MeOH to evaporate to dryness. The sample was exposed to iodine for 4 hrs at 21° C and then the samples were coated with carbon. The sample was analysed by SEM-XRF as described above.

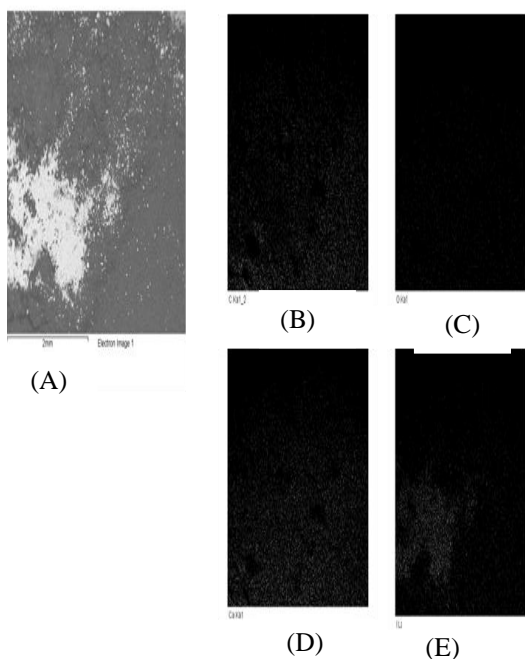


Fig 3. Backscattered electron image of acenaphthylene with calcium carbonate exposed to iodine for 4 hr at 21 °C with magnifications 30x (A). Distribution map of carbon (B), distribution map of oxygen (C), distribution map of calcium (D) and distribution map of iodine (E).

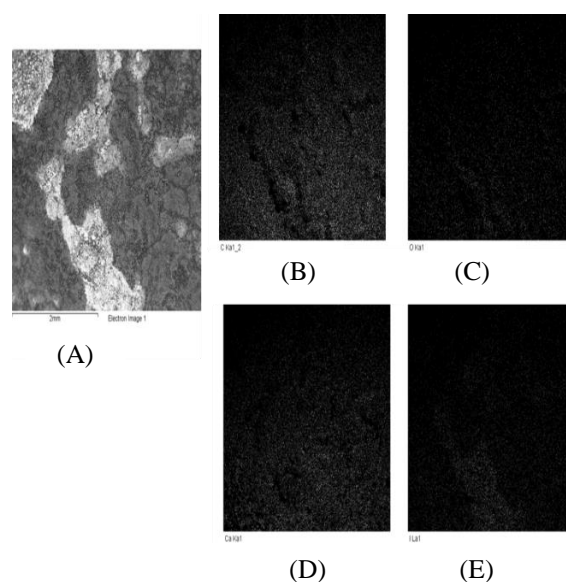


Fig 4. Backscattered electron image of fluorene with calcium carbonate exposed to iodine for 4 hr at 21 °C with magnifications 30x (A). Distribution map of carbon (B), distribution map of oxygen (C), distribution map of calcium (D) and distribution map of iodine (E).

B. Oleic acid to confirm iodine absorption

In this method 0.3 g of oleic acid was weighed into a glass scintillation vial and 1ml of DCM/MeOH 2:1 (v/v) was used to make a solution. 0.5 g of calcium carbonate was weighed in a glass scintillation vial, and 1 ml of the solution of oleic acid then added. The sample was well mixed and left in a fume cupboard to enable the DCM/MeOH to evaporate to dryness. The sample was exposed to iodine for 4 hrs at 21° C and then the samples were coated with carbon. The sample was analysed by SEM-XRF as described above.

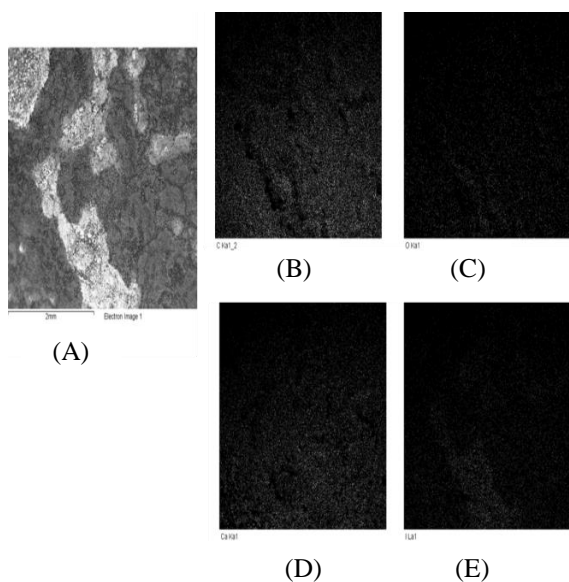


Fig 4. Backscattered electron image of fluorene with calcium carbonate exposed to iodine for 4 hr at 21 °C with magnifications 30x (A). Distribution map of carbon (B), distribution map of oxygen (C), distribution map of calcium (D) and distribution map of iodine (E).

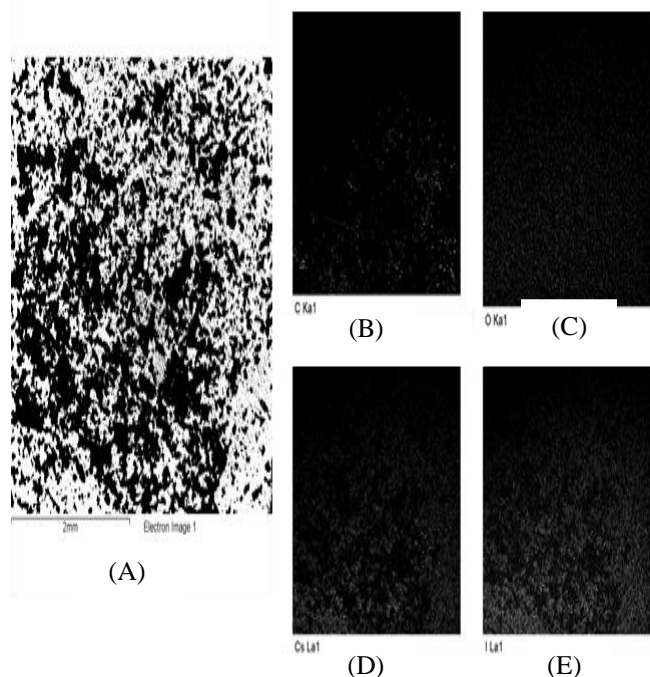


Fig 5. Backscattered electron image of high concentration of oleic acid with calcium carbonate exposed to iodine for 4 hr at 21 °C with magnifications 30x (A). Distribution map of carbon (B), distribution map of oxygen (C), distribution map of calcium (D) and mapping of iodine (E).

C. Using sand instead of calcium carbonate

In this method, sand was used instead of calcium carbonate with fluorene. 1 g of fluorene was weighed in a glass scintillation vial and 4ml of DCM/MeOH 2:1 (v/v) was used to dissolve the fluorene. 0.5 g of sand was weighed in a glass scintillation vial, and 2ml of the solution of fluorenewas then spiked. The sample was well mixed and the sample left in a fume cupboard to enable the DCM/MeOH to evaporate to dryness. The sample exposure to iodine for 4 hr at 21° C. The samples were analysed by SEM-XRF as described above.

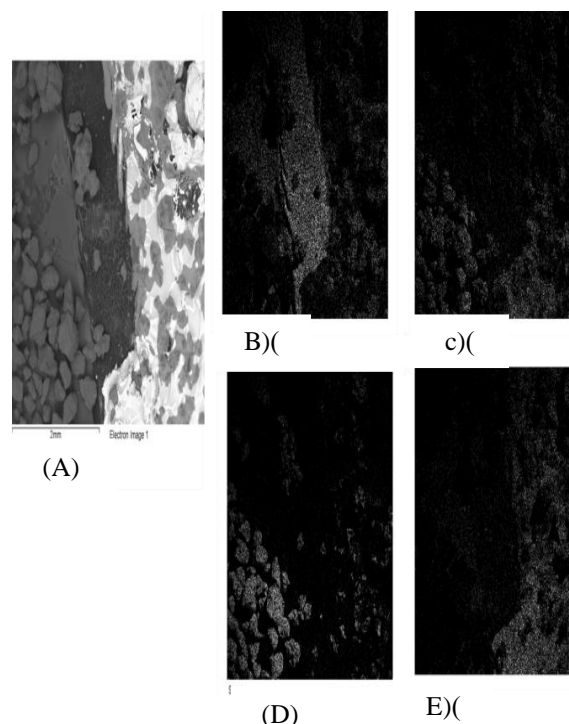


Fig 6. Backscattered electron image of fluorene with sand exposed to iodine for 4 hr at 21 °C with magnifications 30x (A). Distribution map of carbon (B), distribution map of oxygen (C), distribution map of silica (D) and distribution map of iodine (E).

In this method a transparent plastic sleeve was used in which a copy of the relevant image could be placed; then with a ruler, marker pen and set square, a grid was drawn on one side of the sleeve to create 5 x 20 sub-squares, resulting in 100 identical sub-squares. Copies of all the images were then made to the same scale so that comparison could be made, the whole image being covered by the grid, so that the whole of each image could be seen and analysed through the plastic. An evaluation was then made of the number of grid squares that have a lighter colour in them covering at least 50% of the square). Since there were 100 squares, this was then expressed as a percentage. This is equivalent to the 50% Sub-Quadrat Frequency method described in ecological literature when sampling using quadrats (see for example Kershaw, 1973) [10].

IV. RESULTS AND DISCUSSION

Bright areas on backscatter images shown in the sections above indicate the presence of high atomic number elements (iodine in these experiments). Dark region indicate a low concentration. Oleic acid put on to a calcium carbonate substrate shows bright areas in Figure 5. E confirming the presence of iodine and therefore the mechanism of iodine interaction with the unsaturated oleic acid.



Figure 1 (anthracene), Figure 2 (phenanthrene), Figure 3 (acenaphthylene) and Figure 4 (fluorine) show the results when different PAHs are added to calcium carbonate. All shows bright areas in backscattered electron image for iodine (part E of the figures). These results indicate that these PAHs interact with iodine in a similar way to that reported by Goldenberg et al. (2014). This means that iodine can be used as a marker for PAHs and their distribution on mineral surfaces.

Figure 6 shows the results of the interaction of PAH fluorene with sand. Much more limited bright areas are seen in Figure 6. E (iodine) than Figure 4.E, therefore indicating that fluorine does not interact with silica and that the interactions with calcium carbonate are much stronger. Therefore there is an interaction between certain minerals and PAHs.

The images were analysed by using a grid placed over each image to give an estimate of the percentage cover of bright area in each image. The results are shown in Table 1.

Table 1. Estimated Percentages of Bright Areas on XRD Images From Use of The 50% Sub-Quadrat Frequency Method, for Backscattered Electron Images and for Iodine Mapping Images.

Figure Number	Backscattered Electron image	Iodine Mapping
3.9	80%	70%
3.10	75%	60%
3.11	60%	50%
3.12	70%	50%
3.13	80%	65%
3.14	65%	50%

It may be noted that the amount of iodine is estimated to be in larger quantities on the backscattered electron image (A) than for the mapping of iodine (E) in all the Figures.

V. CONCLUSIONS

To sum up all the results, iodine exposure is best at 21 °C. BSE images reveal the presence of iodine, SE and XRF data confirm the present and abundance of iodine (and other elements) but the images are less clear. Higher concentrations and greater time exposure of PAHs increases the absorption of iodine. A magnifications 30x was used because this magnification covers all the surface of a sample but 100 x focuses on a smaller area in the surface of the sample. Oleic acid was used to confirm the result of this experiment as fatty acids have previously been shown to adsorb iodine. All PAHs tested here (acenaphthylene, anthracene, and phenanthrene) adsorb iodine when using a calcium carbonate substrate. Very little PAH adsorbed onto sand (silica).

VI. REFERENCES

- [1] Jiao, W., Lu, Y., Wang, T., Li, J., Han, J., Wang, G. and Hu, W., Polycyclic aromatic hydrocarbons in soils around Guanting Reservoir, Beijing, *China. Chemistry and Ecology*, 25(1), pp.39-48, 2009.
- [2] Yu, X. Z., Gao, Y., Wu, S. C., Zhang, H. B., Cheung, K. C., and Wong, M. H., Distribution of polycyclic aromatic hydrocarbons in soils at Guiyu area of China, affected by recycling of electronic waste using primitive technologies. *Chemosphere*, 65(9), 1500-1509, 2006.
- [3] Kavouras, I.G., Koutrakis, P., Tsapakis, M., Lagoudaki, E., Stephanou, E.G., Von Baer, D. and Oyola, P., Source apportionment of urban particulate aliphatic and polynuclear aromatic hydrocarbons (PAHs) using multivariate methods. *Environmental Science and Technology*, 35(11), pp.2288-2294, 2001.
- [4] Edward, N. T. J., Polycyclic aromatic hydrocarbon (PAHs) in the terrestrial environment- a review. *Journal of Environmental Quality*, 12(4), pp. 427-441, 1983.
- [5] Rey-Salgueiro, L., Martínez-Carballo, E., García-Falcón, M.S. and Simal-Gándara, J., Effects of a chemical company fire on the occurrence of polycyclic aromatic hydrocarbons in plant foods. *Food Chemistry*, 108(1), pp.347-353, 2008.
- [6] Menzie, C.A., Potocki, B.B. and Santodonato, J., Exposure to carcinogenic PAHs in the environment. *Environmental Science and Technology*, 26(7), pp.1278-1284, 1992.
- [7] Madrid, L., Díaz-Barrientos, E. and Madrid, F., Distribution of heavy metal contents of urban soils in parks of Seville. *Chemosphere*, 49(10), pp.1301-1308, 2002.
- [8] Chen, C.W. and Chen, C.F., Distribution, origin, and potential toxicological significance of polycyclic aromatic hydrocarbons (PAHs) in sediments of Kaohsiung Harbour, Taiwan. *Marine Pollution Bulletin*, 63(5-12), pp.417-423, 2011.
- [9] Goldenberg, L., Neumann, R. and Weiner, S., Microscale distribution and concentration of preserved organic molecules with carbon-carbon double bonds in archaeological ceramics: relevance to the field of residue analysis. *Journal of Archaeological Science*, 42, pp.509-518, 2014.
- [10] Kershaw, K. A., Quantitative and Dynamic Plant Ecology 2nd Ed Hodder and Stoughton 1973.